Octave-spanning supercontinuum generation in *in situ* tapered As_2S_3 fiber pumped by a thulium-doped fiber laser

Charles W. Rudy,[1,*] Alireza Marandi,[1] Konstantin L. Vodopyanov,[1,2] and Robert L. Byer[1]

[1]*Edward L. Ginzton Laboratory, Stanford University, 348 Via Pueblo Mall, Stanford, California 94305, USA*

[2]*CREOL, College of Optics & Photonics, University of Central Florida, Orlando, Florida 32816, USA*

**Corresponding author: cwrudy@stanford.edu*

Received May 2, 2013; revised June 28, 2013; accepted July 8, 2013;
posted July 8, 2013 (Doc. ID 189847); published July 30, 2013

We report a supercontinuum spanning well over an octave of measurable bandwidth from about 1 to 3.7 μm in a 2.1 mm long As_2S_3 fiber taper using the *in situ* tapering method. A sub-100-fs mode-locked thulium-doped fiber laser system with ~300 pJ of pulse energy was used as the pump source. Third-harmonic generation was observed and currently limits the pump pulse energy and achievable spectral bandwidth.

OCIS codes: (320.6629) Supercontinuum generation; (060.2390) Fiber optics, infrared.
http://dx.doi.org/10.1364/OL.38.002865

Supercontinuum generation (SCG) has been heralded as a technique for generating a broadband coherent spectrum, useful for many applications, including spectroscopy [1] and ultrashort pulse generation and stabilization [2]. Initially produced in the visible wavelength range, SCG has shifted to longer wavelengths driven by applications in spectroscopy [3,4] and the increased quality and availability of mid-infrared (mid-IR) materials.

A useful mid-IR material for SCG is the chalcogenide As_2S_3, largely due to its low propagation loss, <100 dB/km [5], and high nonlinear index, >200 times that of silica at 1.5 μm [6]. Unfortunately, the zero group velocity dispersion (GVD) point of bulk and single-mode fiber (SMF) As_2S_3 is well into the mid-IR [7], causing available ultrafast pump sources to be in the normal GVD regime. To generate a coherent SC using low pulse energies, it is convenient to use a pump source that is slightly in the anomalous GVD regime, where spectral broadening due to soliton dynamics—mainly soliton fission—can be exploited [8]. In the normal GVD regime, four-wave mixing and Raman scattering contribute to the broadening, leading to higher pulse energies being needed to generate a similar spectral bandwidth as in the case of SCG through soliton fission [8].

Waveguide dispersion can be used to compensate for As_2S_3's material dispersion by shifting the zero GVD wavelength to shorter than available pump wavelength. The waveguide dispersion can be created through fiber tapering [9–11], microstructured optical fibers (MOFs) [12–14], or a combination of the two [15,16]. By using the *in situ* fiber tapering method [17,18] the dispersion can be optimized to generate an efficient SCG in a short fiber taper, which reduces excessive nonlinear processes and improves coherence across the generated spectrum. This allows for spectral broadening of coherent mid-IR frequency combs.

The pump source was an IMRA Tm-doped fiber laser and amplifier system [19], which produced sub-100-fs pulses with an average power of 450 mW at a 75 MHz repetition rate and a center wavelength of 2.04 μm. It was coupled to an As_2S_3 SMF, with a core diameter of 7 μm, cladding diameter of 160 μm, and 0.2 NA. To shift the GVD of the untapered fiber to the anomalous GVD regime, the As_2S_3 fiber would have to be tapered to a diameter around 2 μm, as shown in Fig. 1.

There have been few reported SCG experiments with Tm-doped fiber lasers as the pump source, specifically in tapered fiber. Previously, Tm-doped fiber lasers and amplifiers have been used to pump long lengths (>10 m) of single-mode ZBLAN fiber [20,21] and tapered chalcogenide MOFs [16]. Tapered chalcogenide SMFs have been used with pump sources in the 1.5 μm [11] and 3.1 μm [17] wavelength ranges. Recently, a 2 mm silica-clad As_2S_3 "nanospike" pumped by a Tm-doped fiber laser generated similar spectral bandwidths to the results reported in this Letter [22]. The silica cladding allowed for increased

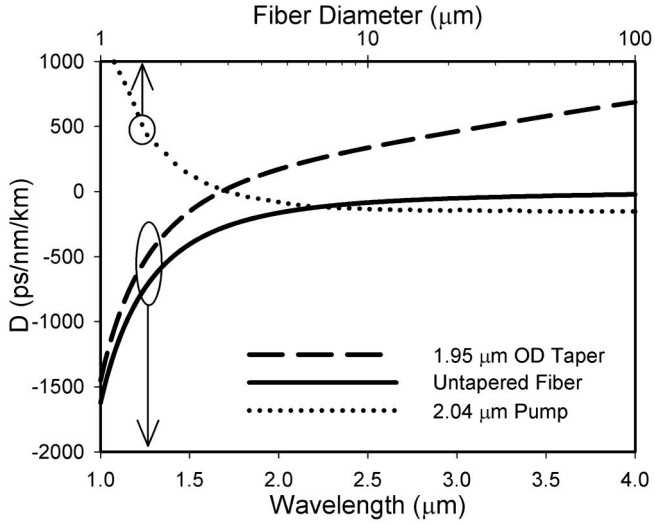

Fig. 1. GVD of the fundamental mode for the untapered fiber (solid) and tapered fiber with ~2 μm diameter (dashed) for varying wavelengths (bottom axis) is shown. The pump wavelength (2.04 μm) experiences normal GVD in the untapered fiber and anomalous GVD once the fiber is tapered. The GVD at the pump wavelength (dotted) is shown for varying fiber taper diameters (top axis) of the order of 1 to 100 μm. The GVD becomes anomalous at fiber diameters below ~3 μm.

mechanical stability, while limiting generation of radiation further into the mid-IR and reducing the coupling efficiency to an optical fiber. By using a Tm-doped fiber laser and an adiabatically tapered fiber, a compact all-fiber SCG source can be optimized.

The *in situ* tapering setup depicted in Fig. 2 is similar to one that has been described in [17,18], where a 3.1 μm ultrafast source was broadened to over an octave—from 2.2 to 5 μm. A resistive heater was constructed from aluminum and cartridge heaters to heat the As_2S_3 SMF to ~200°C, which provided a heat zone length of 2.1 mm. One addition to the previous edition of the *in situ* tapering setup was a temperature sensor permanently attached to the resistive heater block, which helped increase the tapered fiber success rate to ~90% by better monitoring the heater's temperature.

The input (L_1) and output (L_2) lenses consisted of a 12.7 mm focal length 3–5 μm AR-coated aspheric ZnSe lens and a 20 mm focal length plano-convex ZnSe lens, respectively. The collimated output was sent to a monochromator set to the long wavelength edge of the pump spectrum, ~2.2 μm (with ~20 nm bandwidth), to create the spectral measurement signal needed for *in situ* tapering. At this wavelength, the signal of the pump through the untapered fiber was ~6 dB above the noise floor. By temporarily removing a turning mirror on a magnetic base, the output fiber tip could be imaged using a pyroelectric camera to monitor the coupling of the pump source to the fundamental mode of the As_2S_3 fiber. Tapering was achieved using the static tapering method. After the temperature stabilized to 200 ± 0.1°C, the motorized stages began to pull the two ends of the fiber in opposite directions each at 10 μm/s, while the heater remained stationary. This produces an exponential taper shape with a long transition region and a taper waist that is approximately equal to the heat zone [23].

With 450 mW of average output power incident on the input coupling lens, about 90 mW could be coupled through the fiber. The low coupling ratio is due to Fresnel reflections from the high-index As_2S_3 fiber as well as reflections from the input and output coupling lenses. The AR coating for the 3–5 μm wavelength range on L_1 provided large reflections at 2 μm, creating loss close to 30%; however, the excess loss was not an issue, as the input power was limited to well below the available pump power. After accounting for losses, the coupling to the fiber is close to 90%. Even though 90 mW could be coupled to the untapered fiber, the maximum average output power coupled through the tapered fiber was limited to ~15 mW, which corresponds to ~300 pJ of pulse energy within the chalcogenide fiber. During the *in situ* fiber tapering, the average output was maintained at even lower levels, ~5 mW. At higher average pump powers, the tapered fiber would break. It was more susceptible to breakages when heated. The average power (and fluence) observed for taper breakages was lower during the tapering process (5 mW or >20 mJ/cm^2) than after the taper was complete (15 mW or >60 mJ/cm^2). There was only a slight decrease in the power coupled through the fiber after tapering, similar to the results achieved in [17].

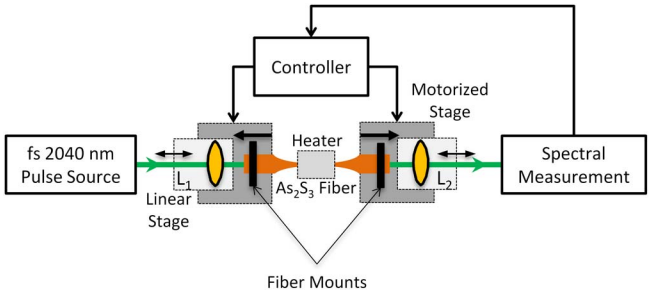

Fig. 2. Setup for the *in situ* fiber tapering system with a 2 μm fs pump source is shown. The motorized stages are used to taper the fiber while the linear stages are used to optimize coupling to the fiber and to the spectral measurement device.

The mechanism for the breakage of the tapered optical fiber most likely comes from third-harmonic generation (THG) in the tapered waist. Visible THG, at a wavelength of ~680 nm, can easily be seen through the scattering from the surface of the tapered region and eventually out of the broken fiber tip. Phase matching for the third harmonic is possible due to intermodal dispersion, where the third harmonic is in a higher-order transverse mode within the multimode taper region of the fiber with a propagation constant equal to that of the fundamental mode at the pump wavelength [24]. The THG is well into the absorptive band of the As_2S_3 fiber; in fact, the ~680 nm light approaches the Urbach absorption edge of the bandgap of As_2S_3 [25]. Therefore, the breakages could be due to direct bandgap absorption generating free carriers, and, in a process similar to the photodarkening effect in doped optical fibers [26], these free carriers could act as broadband absorbers, absorbing the short wavelength side of the SCG. The taper would then break as a result of excessive heating due to the increased absorption. This effect is extremely nonlinear since increasing the pump power would both increase the number of free carriers generated through an increase in THG as well as the spectral power within the absorption spectrum of the free carriers through broadening the output spectrum.

Figure 3 shows the experimental spectral measurement signal during a single tapering experiment, which initially remains unchanged until the pulling length reaches a point where the tapered fiber diameter starts to provide enough waveguide dispersion to create anomalous GVD for the pump (see Fig. 2). Periodic dips in the spectral measurement signal in Fig. 3 are from inspecting the coupling of the pump to the fundamental mode. Due to a decreased mode size in the As_2S_3 SMF compared to the previous *in situ* tapering experiment [17], coupling to the fundamental mode is more sensitive to pointing instabilities that the pump source may have. The peak in the spectral measurement signal occurs at a taper waist diameter of approximately 1.95 μm or a pulling length of about 18.5 mm. This corresponds to a nonlinear coefficient of $\gamma \sim 10\ \mathrm{W^{-1}\,m^{-1}}$ for the 2.1 mm long taper waist. Since the spectral measurement wavelength had to be close to the pump center wavelength (due to the limited pump power used), the spectral measurement signal was less defined than in the previous *in situ* tapered system [17]. For instance, from Fig. 3, a taper diameter variation of 255 nm results in 3 dB decrease of the signal at 2.2 μm—a factor of 2 larger than the previous system—and a 1.78 μm deviation results in 10 dB

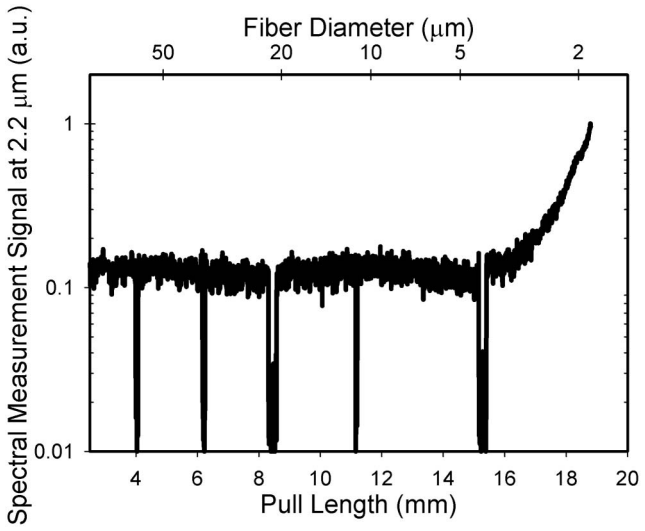

Fig. 3. Output power at 2.2 μm during the tapering process versus the pulling length (bottom axis) and corresponding fiber waist diameter (top axis, log scale). The peak in the spectral measurement signal, at a diameter of 1.95 μm, occurred as the GVD became anomalous as shown in Fig. 1. Dips in the output signal occur due to monitoring of the image of the output fiber tip to ensure coupling to the fundamental mode was maintained.

decrease in the signal at 2.2 μm—a factor of 6 larger than the previous system.

Even with the limited pump power, an extremely broad SC is formed after passing through the short taper waist. Figure 4 shows the SCG spectrum as compared with the original pump spectrum and simulations. The pulse energy coupled into the core of the As_2S_3 fiber was ~300 pJ (or an average output power after the output coupling lens of ~15 mW). The pump spectrum was broadened to cover from ~1 to 3.7 μm (at ~45 dB below the peak) or about 219 THz. The output spectrum

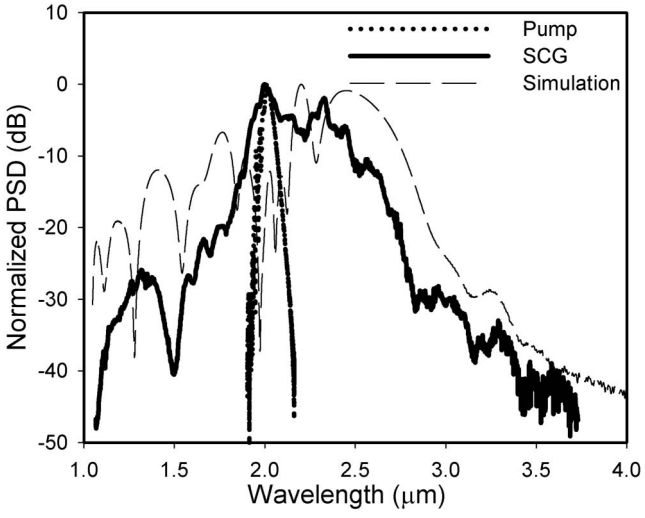

Fig. 4. 2 μm pump spectrum (dotted), the SCG spectrum (solid), and the simulation result (dashed) are shown. The short-wavelength side of the SCG was measured with a Ge detector, the middle of the spectrum with an InSb detector, and the long-wavelength side of the spectrum with a 2.5 μm long-pass filter in place.

spanned an octave at around 25 dB below the peak in the output spectrum. In frequency units, the pump spectral bandwidth was broadened by a factor of 2 at –3 dB, 5 at –10 dB, and 10 at –30 dB. In the simulation (using the method described in [17] with Raman fraction and profile from [27]), a similar spectral bandwidth is generated, with the transform-limited pump pulse first accumulating chirp through propagating in the untapered fiber and taper transition region (with an average dispersion parameter of –135 ps/nm/km calculated from Fig. 1) before it entered the 2.1 mm fiber taper waist. Differences between the simulation and experiment could be due to the grating's uneven spectral response in the measured SCG spectrum as well as additional nonlinear effects outside of the taper region, which were not accounted for in the simulation.

The long-term stability of the As_2S_3 tapers has been studied in our previous work [17], where a fiber taper lasted several months without significant change in the generated spectrum before breaking. Several suggestions for increasing the usable lifetime of these tapers have been presented in [18], including applying an appropriate coating with low loss in the mid-IR or purging the container with dry N_2 to remove moisture.

Alternatively, by optimizing the dispersion of an As_2S_3 MOF, a more mechanically stable structure could be produced. With additional stability, the amount of average power that the tapered fiber could support may increase, allowing for further broadening of the SCG. To further stabilize the system, the tapered As_2S_3 fiber could be butt-coupled or even spliced to the pump source, allowing for the creation of a compact all-fiber mid-IR SCG source while maintaining the properties of the frequency comb pump source.

In conclusion, a substantially broadened SC was generated using the *in situ* fiber tapering method with an ultrafast 2 μm pump source. The measurable output spectrum approached multiple octaves covering the near-IR and extending into the mid-IR from about 1 to 3.7 μm (219 THz). This spectrum was generated in a 2.1 mm long taper with about 300 pJ of pulse energy. Currently, the spectral bandwidth is limited by the amount of average pump power that can be passed through the taper before breaking due to absorption and subsequent heating caused by THG.

The authors would like to acknowledge M. F. Churbanov, G. E. Snopatin, V. G. Plotnichenko, and E. M. Dianov from the Russian Academy of Sciences for providing the As_2S_3 fiber. We also are grateful for support from ONR, NASA, AFOSR, and JTO.

References

1. C. Lin and H. Stolen, Appl. Phys. Lett. **28**, 216 (1976).
2. C. Vozzil, G. Cirmi, C. Manzoni, E. Benedetti, F. Calegari, G. Sansone, S. Stagira, O. Svelto, S. De Silvestri, M. Nisoli, and G. Cerullo, Opt. Express **14**, 10109 (2006).
3. P. S. Monks and K. A. Willis, Educ. Chem. **47**(4), 110 (2010).
4. J. I. Steinfeld and J. Wormhoudt, Annu. Rev. Phys. Chem. **49**, 203 (1998).
5. G. E. Snopatin, V. S. Shiryaev, V. G. Plotnichenko, E. M. Dianov, and M. F. Churbanov, Inorg. Mater. **45**, 1439 (2009).

6. J. S. Sanghera, C. M. Florea, L. B. Shaw, P. Pureza, V. Q. Nquyen, M. Bashkansky, Z. Dutton, and I. D. Aggarwal, J. Non-Cryst. Solids **354**, 462 (2008).
7. W. S. Rodney, I. H. Maliston, and T. A. King, J. Opt. Soc. Am. **48**, 633 (1958).
8. J. M. Dudley and J. R. Taylor, *Supercontinuum Generation in Optical Fibers* (Cambridge University, 2010).
9. T. A. Birks, W. J. Wadsworth, and P. S. J. Russell, Opt. Lett. **25**, 1415 (2000).
10. D.-I. Yeom, E. C. Mägi, M. R. E. Lamont, M. A. F. Roelens, L. Fu, and B. J. Eggleton, Opt. Lett. **33**, 660 (2008).
11. D. D. Hudson, S. A. Dekker, E. C. Magi, A. C. Judge, S. D. Jackson, E. Li, J. S. Sanghera, L. B. Shaw, I. D. Aggarwal, and B. J. Eggleton, Opt. Lett. **36**, 1122 (2011).
12. P. Domachuk, N. A. Wolchover, M. Cronin-Golomb, A. Wang, A. K. George, C. M. B. Cordeiro, J. C. Knight, and F. G. Omenetto, Opt. Express **16**, 7161 (2008).
13. J. Hu, C. R. Menyuk, L. B. Shaw, J. S. Sanghera, and I. D. Aggarwal, Opt. Express **18**, 6722 (2010).
14. M. El-Amraoui, J. Fatome, J. C. Jules, B. Kibler, G. Gadret, C. Fortier, F. Smektala, I. Skripatchev, C. F. Polacchini, Y. Messaddeq, J. Troles, L. Brilland, M. Szpulak, and G. Renversez, Opt. Express **18**, 4547 (2010).
15. M. A. Foster and A. L. Gaeta, Opt. Express **12**, 3137 (2004).
16. M. Duhant, W. Renard, G. Canat, J. Tolès, P. Toupin, L. Brilland, F. Smektala, A. Bétourné, P. Bourdon, and G. Renversez, Proc. SPIE **8237**, 823735 (2012).
17. A. Marandi, C. W. Rudy, V. G. Plotnichenko, E. M. Dianov, K. L. Vodopyanov, and R. L. Byer, Opt. Express **20**, 24218 (2012).
18. C. W. Rudy, A. Marandi, K. L. Vodopyanov, and R. L. Byer, J. Vis. Exp. (75), e50518 (2013).
19. J. Jiang, A. Ruehl, I. Hartl, and M. E. Fermann, in *Proceedings of the Conference on Lasers and Electro-Optics* (Optical Society of America, 2011), paper CThBB5.
20. O. P. Kulkarni, V. V. Alexander, M. Kumar, M. J. Freeman, M. N. Islam, F. L. Terry, Jr., M. Neelakandan, and A. Chan, J. Opt. Soc. Am. B **28**, 2486 (2011).
21. J. Swiderski, M. Michalska, and G. Maze, Opt. Express **21**, 7851 (2013).
22. N. Granzow, M. A. Schmidt, W. Chang, L. Wang, Q. Coulombier, J. Troles, P. Toupin, I. Hartl, K. F. Lee, M. E. Fermann, L. Wondraczek, and P. St. J. Russell, Opt. Express **21**, 10969 (2013).
23. T. A. Birks and Y. W. Li, J. Lightwave Technol. **10**, 432 (1992).
24. T. Lee, Y. Jung, C. A. Codemard, M. Ding, N. G. R. Broderick, and G. Brambilla, Opt. Express **20**, 8503 (2012).
25. J. S. Sanghera and I. D. Aggrawal, J. Non-Cryst. Solids **213–214**, 63 (1997).
26. M. M. Broer, D. M. Krol, and D. J. DiGiovanni, Opt. Lett. **18**, 799 (1993).
27. C. Xiong, E. Mägi, F. Luan, A. Tuniz, S. Dekker, J. S. Sanghera, L. B. Shaw, I. D. Aggarwal, and B. J. Eggleton, Appl. Opt. **48**, 5467 (2009).